Inorg. Chem. **2007**, *46*, 1222−1232

Evidence for Strong Tantalum-to-Boron Dative Interactions in $(silox)_3Ta(BH_3)$ and $(silox)_3Ta(\eta^2\text{-B,Cl-}BCl_2Ph)$ (silox = ^{t}Bu$_3$SiO)[1]

Jeffrey B. Bonanno,[†] Thomas P. Henry,[†] Peter T. Wolczanski,*[,†] Aaron W. Pierpont,[‡] and Thomas R. Cundari*[,‡]

Department of Chemistry and Chemical Biology, Baker Laboratory, Cornell University, Ithaca, New York 14853, and Department of Chemistry, Center for Advanced Scientific Computing and Modeling (CASCaM), University of North Texas, Denton, Texas 76203-5070

Received September 6, 2006

Treatment of $(silox)_3Ta$ (**1**, silox = ^{t}Bu$_3$SiO) with BH_3•THF and BCl_2Ph afforded $(silox)_3Ta(BH_3)$ (**2**) and $(silox)_3Ta(\eta^2\text{-B,Cl-}BCl_2Ph)$ (**3**), which are both remarkably stable Ta(III) compounds. NMe_3 and ethylene failed to remove BH_3 from **2**, and no indication of BH_3 exchange with BH_3·THF-d_8 was noted via variable-temperature ^{1}H NMR studies. Addition of BH_3·THF to $(silox)_3TaH_2$ provided the borohydride-hydride $(silox)_3HTa(\eta^3\text{-}BH_4)$ (**5**), and its thermolysis released H_2 to generate **2**. Exposure of **2** to D_2 enabled the preparation of isotopologues $(silox)_3Ta(BH_{3-n}D_n)$ (n = 0, **2**; 1, **2**-D; 2, **2**-D_2; 3, **2**-D_3) for isotopic perturbation of chemical shift studies, but these failed to distinguish between "inverse adduct" (i.e., $(silox)_3Ta{\rightarrow}BH_3$) or $(silox)_3Ta(\eta^2\text{-B,H-}BH_3)$ forms of **2**. Computational models $(RO)_3Ta(BH_3)$ (R = H, **2′**; SiH_3, **2**^{SiH} $SiMe_3$, **2**^{SiMe}, and Si^{t}Bu$_3$, **2**^{SiBu}) were investigated to assess the relative importance of steric and electronic effects on structure and bonding. With small R, η^2-B,H structures were favored, but for **2**^{SiMe} and **2**^{SiBu}, the dative structure proved to be similar in energy. The electonic and vibrational features of both structure types were probed. The IR spectrum of **2** was best matched by the η^2-B,H conformer of **2**^{SiBu}. In related computations pertaining to **3**, small R models favored the oxidative addition of a BCl bond, while with R = Si^{t}Bu$_3$ (**3**^{SiBu}), an excellent match with its X-ray crystal structure revealed the critical steric influence of the silox ligands.

Introduction

Transition metal complexes are usually comprised of ligands, both charged and neutral, that donate pairs of electrons to the more electropositive metal, i.e., $X^-/L{\rightarrow}M$.[2] In principle, electronic deficient groups can also be used to accept electron density from the metal in forming the metal−ligand bond. While this is common for π-interactions—hence the term "π-backbonding" for describing π-bonds in CO, CN^-, olefins, etc.[2]—it is quite unusual for a group to act as a σ-acceptor in the same vein.

Ligands whose core atom violates the octet rule have the greatest potential to interact in a σ-accepting fashion, and BX_3 (X = halide, etc.) or BR_3 (R = H, alkyl, etc.) are likely candidates. In fact, there are a number of isolable late metal compounds claimed to possess purely dative interactions of the $L_nM{\rightarrow}BX_3/R_3$ type,[3] including $[Et_4N][Mn(BH_3)(CO)_4\text{-}PPh_3]$,[4] $Ir\{B(C_6F_5)_3\}(CO)Cl(PEt_3)_2$, and $[trans\text{-}Rh(BF_3)_2(diphos)_2][BPh_4]$.[5] Unfortunately, the lack of structural data pertaining to these adducts has called their bonding descriptions into question.

Adducts of the type $L_nM{\rightarrow}(HBX_2)$ have been prepared and structurally characterized, but in all cases there is an interaction with the hydrogen. In cases where the L_nM fragment is 16e$^-$, the bonds have been construed as "normal" dative interactions—ones in which the H−B electron pair

* To whom correspondence should be addressed. E-mail: ptw2@cornell.edu (P.T.W.).
† Cornell University.
‡ University of North Texas.

(1) Taken in part from: Bonanno, J. B., Ph.D. Thesis, Cornell University, 1996.
(2) Collman, J. P.; Hegedus, L. S.; Norton, J. R.; Finke, R. G. *Principles and Applications of Organotransition Metal Chemistry*; University Science Books: Sausilito, CA, 1987.
(3) Gilbert, K. B.; Boocock, S. K.; Shore, S. G. In *Comprehensive Organometallic Chemistry*; Wilkinson, G.; Stone, F. G. A.; Abel, E. W., Eds.; Pergamon: Oxford, 1982; Vol. 6, Chapter 41.
(4) Parshall, G. W. *J. Am. Chem. Soc.* **1964**, *86*, 361−364.
(5) (a) Scott, R. N.; Shriver, D. F.; Vaska, L. *J. Am. Chem. Soc.* **1968**, *90*, 1079−1080. (b) Scott, R. N.; Shriver, D. F.; Lehmann, D. D. *Inorg. Chim. Acta.* **1970**, *4*, 73−78. (c) Lehmann, D. D.; Shriver, D. F. *Inorg. Chem.* **1974**, *13*, 2203−2207.

10.1021/ic0616885 CCC: $37.00
Published on Web 01/24/2007

donates to the metal center[6]—but the boron atoms are typically well within bonding distance, and the stability of these complexes suggests that metal donation to boron is an integral part of the bonding, i.e., 3-center-4-electron bonding. Depending on metal and environment, the interactions can range from being dominated by H−B donation to the formation of boryl-hydrides with[7,8] or without[9] a long distance H···B remnant. Other examples reveal additional diversity. For the 14e$^-$ bent sandwich fragment Cp_2Ti, two catecholborane ligands appear to bind via their BH bonds, i.e., $Cp_2Ti(\eta^2$-H,B-$HB(O_2C_6H_4))_2$, but there are 6e$^-$ and 5 atoms involved in the bonding, and a rudimentary MO assessment suggests titanium donation to both borons in a single molecular orbital.[10] Isotopic perturbation of chemical shift[11] studies have suggested that $Cp_2Nb(H_2B$(catechol)) exists in solution as an equilibrium between hydrido-borane and borohydride forms, while crystallographic studies showed a single species that appeared to reside on the structural continuum between these limiting cases.[12,13] In very few instances is the boron so distant from the transition metal that it is more correctly described as a bridging hydride in a 3-center-2-electron bond.[14]

$L_nM\rightarrow BX_3$ interactions devoid of any ambiguity regarding η^2-B,H or bridging atoms have recently been observed via BH bond activation of the tris(2-mercapto-1-*R*-imidazolyl)-hydroborato ligand ($HB(mim^R)_3$) to afford metalaboratrane and related complexes. In such derivatives as $\{\kappa^4$-$B(mim^{tBu})_3\}$-$Fe(CO)_2$,[15] $\{\kappa^4$-$B(mim^{Me})_3\}M(CO)PPh_3$ (M = Ru,[16] Os),[17] $[\{\kappa^4$-$B(mim^{tBu})_3\}Co(PPh_3)]BPh_4$,[18] $\{\kappa^4$-$B(mim^R)_3\}M(Cl)PPh_3$ (R = Me, M = Rh;[19] R = ^{t}Bu, M = Rh, Ir),[20] $[\{\kappa^4$-$B(mim^{Me})_3\}Rh(CNR)PPh_3]Cl$,[19] $[\{\kappa^4$-$B(mim^{Me})_3\}Rh(PMe_3)_2]$-Cl,[19] $\{\kappa^3$-S,S,B-$B(mim^R)_3\}Ir(CO)(PPh_3)H$ (R = Me,[21] Ph, ^{t}Bu),[20] $[\{\kappa^4$-$B(mim^{Me})_3\}Pt(PPh_3)H]Cl$, and $\{\kappa^4$-$B(mim^{Me})_3\}$-$Pt(PPh_3)$,[22] the boron is centered over the metal by the three chelate mercaptoimidazole arms of the tripod in the κ^4-arrangement and two in the κ^3-form. Parkin has reviewed these species and has painstakingly delineated the bonding in the pseudo-d^8 Rh and Ir compounds through calculations and by clearly defining valence and d^n, where n = no. valence electrons(neutral atom) − valence. The latter circumvents discrepancies in rationalizing common structure types vs d^n when the oxidation state formalism is mistakenly utilized,[23] which is a problem for $L_nM\rightarrow BX_3$ species, given the neutral view of the metal−boron interaction.

The synthesis of $(silox)_3Ta(BH_3)$ (**2**, silox = ^{t}Bu$_3$SiO), an isotopic perturbation of chemical shift study, derivatives, and calculations are reported herein. The unique structural features of the siloxide ligand apparently sway the bonding of the borane toward the "inverse adduct" or $Ta\rightarrow BH_3$ structure, although it is still possible that the alternative $Ta\rightarrow B(\mu$-$H)H_2$ structure represents the true ground state. A related η^2-B,Cl configuration is found in $(silox)_3Ta(\eta^2$-B,Cl-$BCl_2Ph)$ (**3**).

Results

Boron Adducts of (silox)$_3$Ta. 1. Synthesis. As Scheme 1 indicates, treatment of diethyl ether solutions of $(silox)_3Ta$ (**1**)[24] with excess BH_3·THF (1 M in THF) at −78 °C resulted in an immediate color change from blue to orange. The BH_3 adduct $(silox)_3Ta(BH_3)$ (**2**) was isolated from hexane solution as orange crystals in 67% yield. The ^{1}H NMR spectrum of **2** in benzene-d_6 exhibited a sharp resonance at δ 1.28 and a broad 1:1:1:1 quartet at δ 3.93 ($^1J_{BH}$ = 98 Hz) in a ratio of 27:3, while the ^{11}B NMR spectrum revealed a 1:3:3:1 quartet at δ 27.89 ($^1J_{BH}$ = 98 Hz).[25] Single-frequency decoupling of ^{11}B collapsed the proton signal to a sharp singlet. The infrared spectrum of **2** in nujol revealed two terminal BH stretching absorptions at ν_{BH} = 2445 and 2395 cm^{-1}, and a weak absorption at 1290 cm^{-1} attributed to BH bending.[25] In order to corroborate these assignments, a THF solution of **1** was treated with 0.5 equiv of B_2D_6 (presumably generating BD_3·THF in situ) to provide $(silox)_3Ta(BD_3)$ (**2**-D_3). Its IR spectrum (nujol) manifested sharp absorptions at 1845 and 1770 cm^{-1} (ν_{BH}/ν_{BD} = 1.32 and 1.35, respectively) accompanied by a weak absorption at 980 cm^{-1} (ν_{BH}/ν_{BD} = 1.32). The ratios are in good agreement with the value predicted by a reduced mass calculation (ν_{BH}/ν_{BD} = 1.36)[26] and are therefore considered simple BH vibrations without strong coupling to other modes. The spectral characterizations

(6) Schlecht, S.; Hartwig, J. F. *J. Am. Chem. Soc.* **2000**, *122*, 9435−9443.
(7) (a) Lantero, D. R.; Miller, S. L.; Cho, J. Y.; Ward, D. L.; Smith, M. R., III. *Organometallics* **1999**, *18*, 235−247. (b) Lantero, D. R.; Ward, D. L.; Smith, M. R., III. *J. Am. Chem. Soc.* **1997**, *119*, 9699−9708. (c) Lantero, D. R.; Motry, D. H.; Ward, D. L.; Smith, M. R., III. *J. Am. Chem. Soc.* **1994**, *116*, 10811−10812.
(8) Hartwig, J. F.; Cook, K. S.; Hapke, M.; Incarvito, C. D.; Fan, Y. B.; Webster, C. E.; Hall, M. B. *J. Am. Chem. Soc.* **2005**, *127*, 2538−2552.
(9) Hartwig, J. F.; He, X. M. *Organometallics* **1996**, *15*, 5350−5358.
(10) (a) Muhoro, C. N.; He, X. M.; Hartwig, J. F. *J. Am. Chem. Soc.* **1999**, *121*, 5033−5046. (b) Hartwig, J. G.; Muhoro, C. N. *Organometallics* **2000**, *19*, 30−38.
(11) (a) Saunders, M.; Telkowski, L.; Kates, M. R. *J. Am. Chem. Soc.* **1977**, *99*, 8070−8071. (b) Saunders, M.; Kates, M. R. *J. Am. Chem. Soc.* **1977**, *99*, 8071−8072. (c) Saunders, M.; Kates, M. R.; Wiberg, K. B.; Pratt, W. *J. Am. Chem. Soc.* **1977**, *99*, 8072−8073.
(12) Hartwig, J. F.; De Gala, S. R. *J. Am. Chem. Soc.* **1994**, *116*, 3661−3662.
(13) Jensen, J. A.; Wilson, S. R.; Girolami, G. S. *J. Am. Chem. Soc.* **1988**, *110*, 4977−4982.
(14) Shimoi, M.; Nagai, S.; Ichikawa, M.; Kawano, Y.; Katoh, K.; Uruichi, M.; Ogino, H. *J. Am. Chem. Soc.* **1999**, *121*, 11704−11712.
(15) Figueroa, J. S.; Melnick, J. G.; Parkin, G. *Inorg. Chem.* **2006**, *45*, 7056−7058.
(16) Foreman, M. R. St.-J.; Hill, A. F.; Owen, G. R.; White, A. J. P.; Williams, D. J. *Organometallics* **2003**, *22*, 4446−4450.
(17) Foreman, M. R. St.-J.; Hill, A. F.; White, A. J. P.; Williams, D. J. *Organometallics* **2004**, *23*, 913−916.
(18) Mihalcik, D. J.; White, J. L.; Tanski, J. M.; Zakharov, L. N.; Yap, G. P. A.; Incarvito, C. D.; Rheingold, A. L.; Rabinovich, D. *Dalton Trans.* **2004**, 1626−1634.
(19) Crossley, I. R.; Hill, A. F.; Willis, A. C. *Organometallics* **2006**, *25*, 289−299.
(20) Landry, V. K.; Melnick, J. G.; Buccella, D.; Pang, K.; Ulichny, J. C.; Parkin, G. *Inorg. Chem.* **2006**, *45* 2588−2597.
(21) Crossley, I. R.; Hill, A. F.; Willis, A. C. *Organometallics* **2005**, *24*, 1062−1064.
(22) Crossley, I. R.; Hill, A. F. *Organometallics* **2004**, *23*, 5656−5658.
(23) (a) Parkin, G. *J. Chem. Educ.* **2006**, *83*, 791−799. (b) Parkin, G. *Organometallics* **2006**, *25*, 4744−4747.
(24) Neithamer, D. R.; LaPointe, R. E.; Wheeler, R. A.; Richeson, D. S.; Van Duyne, G. D.; Wolczanski, P. T. *J. Am. Chem. Soc.* **1989**, *111*, 9056−9072.
(25) Marks, T. J.; Kolb, J. R. *Chem. Rev.* **1977**, *77*, 263−293.
(26) Silverstine, R. M.; Bassler, G. C.; Morrill, T. C. *Spectrometric Identification of Organic Compounds*; John Wiley and Sons: New York, 1981; Chapter 3.

Scheme 1

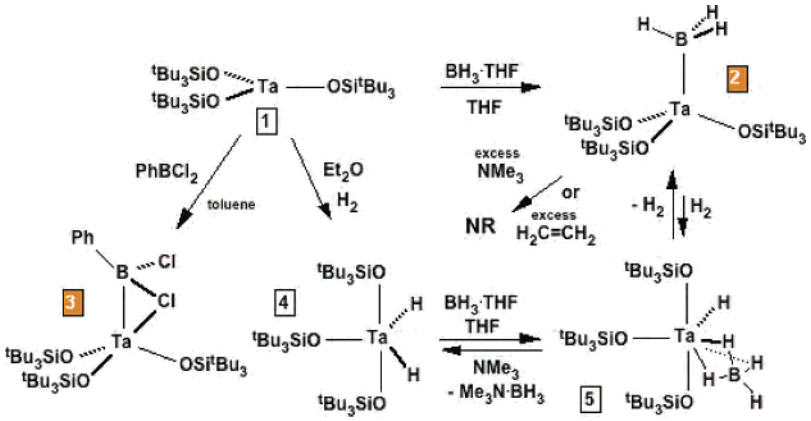

suggested that **2** was an "inverse adduct" of the type $(silox)_3Ta{\rightarrow}BH_3$, but the possibility of a Ta···H···B interaction(s) remained.

The BH_3 ligand of **2** is strongly bound to tantalum and is quite inert. When **2** was heated in benzene-d_6 at 90 °C for 24 h, no decomposition was noted. Under similar conditions, **2** was treated with 3 equiv of C_2H_4, but there was no evidence of any BEt groups, which would have been expected if BH_3 had been liberated.[27] In the presence of ~10 equiv of NMe_3, no degradation of **2** was noted after a week at 23 °C.[28] Exchange experiments between **2** and BH_3·THF in THF-d_8 (1:1, 0.029 M) were monitored by ^{11}B NMR spectroscopy, and no hint of line broadening (toward coalescence) was observed up to 80 °C, placing a very conservative lower limit on dissociative (or pseudo-dissociative) exchange at >19 kcal/mol. Even in a donor solvent (THF) that could facilitate BH_3 loss in an associative (pseudo-dissociative in the case of a donor solvent) fashion, the BH_3 unit appears to to be very difficult to remove. This is best rationalized in terms of thermodynamic stability.

Efforts to extend the range of these adducts to include BR_3 (R = Me, Ph) species failed, with no noticeable binding detected, and simple HBR_2 and H_2BR species were avoided due to probable complications from H/R exchange. Instead, **1**[24] was treated with 1 equiv of $PhBCl_2$ at 23 °C in toluene (Scheme 1), and the solution quickly turned from blue to deep red. The addition of hexane at −78 °C precipitated orange crystals of $(silox)_3Ta(\eta^2\text{-B,Cl-}BCl_2Ph)$ (**3**) in 69% yield. In C_6D_6, the ^1H NMR spectrum of **3** displayed a sharp singlet at δ 1.26 and three aryl resonances in a 1:2:2 ratio. Three aryl $^{13}C\{^1H\}$ NMR spectral resonances were observed in THF-d_8; presumably the ipso resonance (B*C*) was too broadened by ^{11}B coupling (^{11}B, $I = 3/2$, 80%; ^{10}B, $I = 3$, 20%) to be clearly seen. While the oxidative addition of a B−Cl bond was considered, these bonds are quite strong, and the orange color of **3** belied this possibility since most Ta(V) species characterized in this system are colorless. The orange color was consistent with a dative interaction (i.e., $(silox)_3Ta{\rightarrow}BCl_2Ph$), but assignment of ν(BCl) bands[29] in the IR proved to be difficult due to overlapping siloxide absorptions. Without IR data pertaining to BCl connectivity, it was not possible to unambiguously assign a structure to **3**, especially with the potential for μ-Cl interactions. Thermolysis of **3** at 60 °C for 2 days afforded $(silox)_3TaCl_2$[24] as ~60−70% of the product mixture, and the fate of the PhB fragment was undetermined.

2. Structure of $(silox)_3Ta(\eta^2\text{-B,Cl}-BCl_2Ph)$. A single-crystal X-ray structure determination of **3** revealed an η^2-B,Cl binding mode in the pseudo-tetrahedral structure illustrated in Figure 1. The d(B1−Cl1) distance of 1.999(8) Å is markedly longer than its terminal partner (i.e., B1−Cl2), which is 1.828(8) Å. The Ta−B1−Cl1 plane is directly aligned with the Ta−O3 bond and bisects the O1−Ta−O2 angle (i.e., ∠Cl1−Ta−O1 = 87.65(14)°, ∠Cl1−Ta−O2 = 87.74(14)°). Steric and electronic influences of Cl1 provide a reason for the greater spread of ∠O1−Ta−O2 (123.5(2)°) relative to ∠O1−Ta−O3 (105.4(2)°) and ∠O2−Ta−O3 (106.6(2)°). The Ta→B dative interaction of 2.308(8) Å is significantly longer than the sum of covalent radii (r_{Ta} = 1.34 Å, r_B = 0.82 Å, $\sum(r_{Ta} + r_B)$ = 2.16 Å), perhaps due to the strain induced by the Ta−Cl1 interaction of 2.561 Å, which is also substantially longer than a normal covalent bond (r_{Cl} = 0.99 Å, $\sum(r_{Ta} + r_{Cl})$ = 2.33 Å). The Ta−B1 interaction clearly perturbs the planarity about boron, since the ∠Cl1−B−Cl2 (107.5(4)°), ∠C1−B−Cl2 (114.4(5)°), and ∠C1−B−Cl1 (110.9(5)°) angles sum to only 332.8°. Note that the boron is close to occupying a regular position in a tetrahedron, since the ∠B1−Ta−O3 angle of 101.2(2)° is only somewhat less than the ∠B1−Ta−O1 and ∠B1−Ta−O2 angles of 108.4(2)° and 109.4(2)°, respectively.

Borohydride $(silox)_3HTa(\eta^3\text{-}BH_4)$. 1. Synthesis. When $(silox)_3TaH_2$ (**4**), generated from dihydrogen and **1** in diethyl ether,[30] was exposed to 1 equiv of BH_3·THF at 23 °C, the colorless borohydride complex $(silox)_3HTa(\eta^3\text{-}BH_4)$ (**5**) was isolated in 77% yield (Scheme 1). The ^1H NMR spectrum of **5** consisted of a singlet at δ 1.29 corresponding to the

(27) Zaidlewicz, M. In *Comprehensive Organometallic Chemistry*; Wilkinson, G., Stone, F. G. A., Abel, E. W., Eds.; Pergamon: Oxford, 1982; Vol. 7, Chapter 45.2.

(28) For, example, NMe_3 abstracts 1 or 2 equiv BH_3 from $Cp_2Zr(BH_4)_2$ to yield the hydride/borohydride or dihydride complexes: James. B. D.; Nanda, R. K.; Wallbridge, M. G. H. *Inorg. Chem.* **1967**, *6*, 1979−1983.

(29) Nakamoto, K. *Infrared and Raman Spectra of Inorganic and Coordination Compounds*; Wiley: New York, 1986.

(30) Miller, R. L.; Toreki, R.; LaPointe, R. E.; Wolczanski, P. T.; Van, Duyne, G. D.; Roe, D. C. *J. Am. Chem. Soc.* **1993**, *115*, 5570−5588.

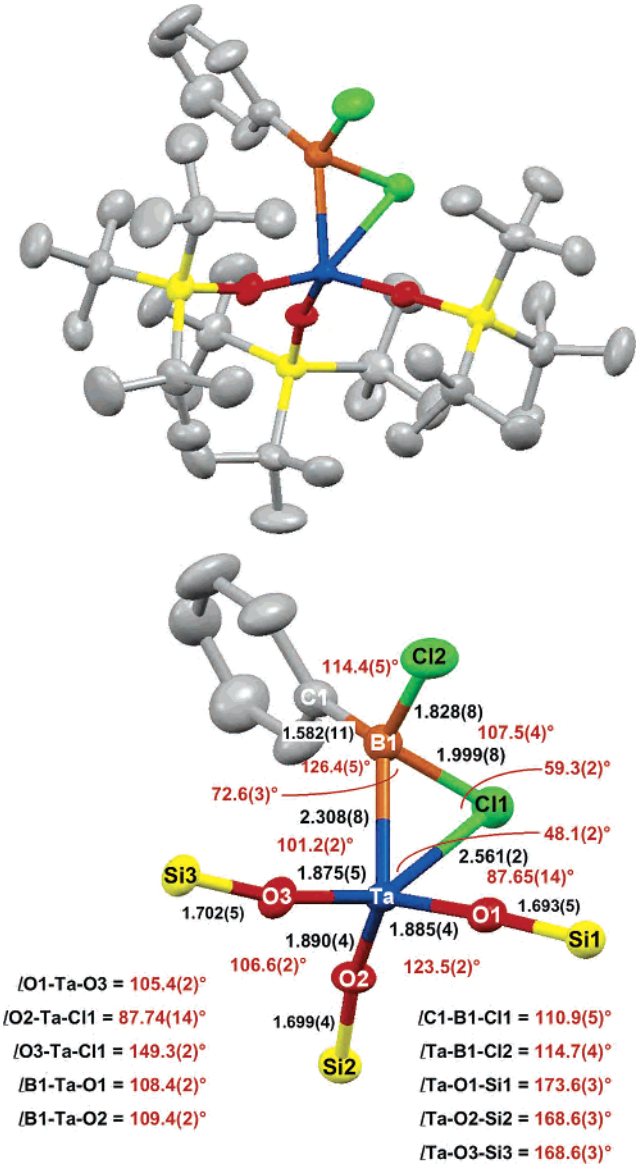

Figure 1. Molecular and core illustrations of (silox)$_3$Ta(η^2-B,Cl-BCl$_2$Ph) (**3**). Bond distances (Å) are in black and bond angles (deg) in red. Interatomic distances (Å): d(Ta−C1) = 3.486(11), d(Ta−Cl2) = 3.493(4).

silox ligand, a broad downfield quintet at δ 22.47 (J_{HH} = 12 Hz) characteristic of the hydride, and a broad unresolved 1:1:1:1 quartet at δ 3.48 that sharpened at 50 °C to enable identification of a $^1J_{BH}$ of 88 Hz. A quintet in the ^{11}B NMR spectrum at δ −16.72 also displayed the 88 Hz coupling. Rapid interconversion of bridging and terminal hydrogens on the NMR time scale is common in a borohydride ligand,[25,31] hence the observation of equivalent hydrogens on boron.

One absorption at 2495 cm^{-1} in the terminal BH stretching region of the IR spectrum, two in the BH bridging region (2200, 2150 cm^{-1}) and another broad weak absorption at 1160 cm^{-1}, which was tentatively assigned to a BH bridge

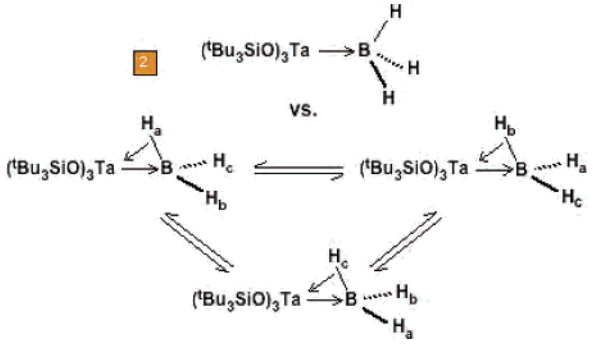

Figure 2. Possible "inverse adduct" and η^2-B,H structures for (silox)$_3$Ta-(BH$_3$) (**2**).

deformation, were characteristic of the η^3-borohydride ligand.[25] A strong band at 1765 cm^{-1} was assigned to the ν(TaH). Treatment of (silox)$_3$TaD$_2$ (**4**-D$_2$) with B$_2$D$_6$ in THF afforded (silox)$_3$DTa(η^3-BD$_4$) (**5**-D$_5$), which exhibited borohydride absorptions at 1870, 1630, and 1580 cm^{-1} corresponding to BD stretching in accord with ν_{BH}/ν_{BD} ratios of 1.33, 1.35, and 1.36, respectively. The ν(TaD) appeared at 1270 cm^{-1} (ν_{BH}/ν_{BD} = 1.39).

2. Equilibration with (silox)$_3$Ta(BH$_3$). In contrast to **2**, exposure of **5** to 1 equiv of NMe$_3$ at 23 °C for ∼3 h completely regenerated dihydride **4** with concomitant formation of Me$_3$N·BH$_3$.[28] The reversibility of η^3-BH$_4$ formation was expected, but the thermal instability of **5** proved to be due to H$_2$ loss and not loss of BH$_3$. White crystals of **5** stored at 25 °C for a number of weeks discolored and **2** was observed in the ^{11}B NMR spectrum of the resulting material. When **5** was heated under ∼3 atm of D$_2$ (90 °C, 18 h), **2**, (silox)$_3$Ta(BH$_2$D) (**2**-D), (silox)$_3$Ta(BHD$_2$), and (silox)$_3$Ta-(BD$_3$) were observed (IR, NMR, vide infra). The addition of H$_2$ (∼3 atm) to solutions of **2** at 90 °C established an equilibrium with **5**. Since **4** rapidly undergoes σ-bond metathesis with D$_2$ to afford (silox)$_3$TaHD (**4**-D) and **4**-D$_2$,[30] it is plausible that H/D exchange in **5** occurs via BH$_3$ loss. However, the conversion of **2** to **5** under H$_2$ (and reverse process in the solid state) suggests that there may be a direct process involving an H$_2$/D$_2$ addition across the Ta−B bond of **2**, and the reverse H$_2$/HD/D$_2$ elimination from isotopomers of **5**.

Isotopic Perturbation of Chemical Shift Studies on (silox)$_3$Ta(BH$_3$). The spectral characterization of **2** is consistent with a symmetric C_{3v} adduct containing a Ta→B dative interaction—an "inverse adduct". However, an η^2-B,H[32] structure where rapid interconversion of the three configurations illustrated in Figure 2 averages the bridge and terminal boron hydride positions is certainly feasible. The IR spectra for such species should have two bands in the terminal BH stretching region and one in the bridging region. The IR spectra do effectively rule out the possibility of rapidly exchanging (silox)$_3$HTaBH$_2$ structures, since an intense ν(TaH) absorption band is absent. The two bands observed in the IR spectrum of **2** may account for the terminal stretching absorptions, while a bridging stretch may be broad and weak and thus difficult to observe. NMR

(31) For, a classic example where terminal/bridged hydrogen exchange is slow (Cp$_2$V(η^2-BH$_4$), $\Delta G^{\ddagger}_{ex}$(−87 °C) ≈ 8 kcal/mol) on the NMR timescale, see: Marks, T. J.; Kennelly, W. J. *J. Am. Chem. Soc.* **1975**, *97*, 1439−1443.

(32) Brookhart, M.; Green, M. L. H. *J. Organomet. Chem.* **1983**, *250*, 395.

spectral techniques for detecting such species include variable-temperature acquisition and the isotopic perturbation of chemical shifts.[12] $^1H\{^{11}B\}$ NMR spectra of **2** obtained in THF-d_8 from 22 to −105 °C showed a single B−H signal that shifts slightly ($\Delta\delta = -0.1$) and only broadens noticeably at −90 °C. Although these results also point to a static C_{3v} structure, interconversion of η^2-B,H-bridging and terminal BH positions is expected to have a very small barrier and may still be rapid at the lowest accessible temperature for this experiment.

Originally applied in carbocation chemistry,[12] isotopic perturbation of chemical shift (initially isotopic perturbation of resonance (IPR)) experiments were first successfully employed in an organometallic system by Shapley et al.,[33] who used it to deduce the η^2-C,H-bridge of a methyl group in $HOs_3(CO)_{10}(\mu_{1,2}$-H,C-$CH_3)$. The experiment takes advantage of the greater propensity of deuterium to reside in terminal sites due to their greater zero point energy vs that of a bridging site. The analogy to the plausible $(silox)_3Ta(\eta^2$-B,H-$BH_3)$ structure of **2** is clear; in a set of isotopologues $(silox)_3Ta(BH_xD_{3-x})$, the deuterium should prefer the terminal sites, and if the intrinsic ^1H chemical shift difference between the bridging and terminal sites is sufficient, the experiment could provide proof of the η^2-B,H structure. If the symmetric, dative structure is the ground state, the ^1H NMR signals of each $(silox)_3Ta(BH_xD_{3-x})$ should be shifted upfield by small increments due to subtle changes in magnetic environment.[34]

A sample for isotopic perturbation of chemical shift study was prepared by thermolysis of **2** in C_6D_6 under ∼3 atm of D_2 for 18 h. Inspection of the $^1H\{^{11}B\}$ NMR spectrum of this sample revealed resonances at δ 3.930, 3.905, and 3.880 that were attributed to **2**, **2**-D, and **2**-D_2. HD coupling was obscured in this experiment as a result of boron decoupling, and neither J_{HD} nor J_{BH} values could be extracted from the corresponding ^1H NMR spectrum due to the broad line widths of the overlapping quartets. Immediately, the validity of the isotopic perturbation of chemical shift experiment was called into question due to the proximity of the three chemical shifts, but the analysis was carried out to completion.

The equilibrating η^2-B,H structures could have small or large shifts upfield or downfield depending on the associated equilibrium constants and the shifts of the terminal and bridging positions. The equilibria and pertinent equations for the chemical shift analysis are given in eqs 1−5, where the δ_t and δ_b subscripts indicate intrinsic terminal and bridge shifts, and δ_n ($n = 0-2$) is the average chemical shift for a particular number of deuteriums. The equations present four unknowns (δ_t, δ_b, K_1, and K_2) and three

$$(silox)_3Ta(\eta^2\text{-B,H}_b\text{-B(H}_t)_2)\ (\mathbf{2})\ \text{has}\ \delta_0 = (2\delta_t + \delta_b)/3 \qquad (1)$$

$$(silox)_3Ta(\eta^2\text{-B,H}_b\text{-B(H}_t)(D_t))\ (\mathbf{2}\text{-D}_t) \overset{K_1}{\rightleftharpoons} (silox)_3Ta(\eta^2\text{-B,D}_b\text{-B(H}_t)_2)\ (\mathbf{2}\text{-D}_b) \qquad (2)$$

$$\delta_1 = (2K_1\delta_t + \delta_t + \delta_b)/(2K_1 + 2) \qquad (3)$$

$$(silox)_3Ta(\eta^2\text{-B,H}_b\text{-B(D}_t)_2)\ (\mathbf{2}\text{-(D}_t)_2) \overset{K_2}{\rightleftharpoons} (silox)_3Ta(\eta^2\text{-B,D}_b\text{-B(H}_t)(D_t))\ (\mathbf{2}\text{-D}_b\text{D}_t) \qquad (4)$$

$$\delta_1 = (K_2\delta_t + \delta_b)/(K_2 + 1) \qquad (5)$$

observables (δ_0, δ_1, and δ_2), but if the "primary" equilibrium isotope effects for K_1 and K_2, i.e., the bridge vs terminal positioning of H vs D, are considered the same and the secondary equilibrium isotope effects (H vs D in the adjacent terminal position) are considered negligible or the same,[35] then $K_2 = 4K_1$. Unfortunately, the fact that $\delta_0 - \delta_1 = 0.025$ ppm is equal to $\delta_1 - \delta_2$ imparts conlinearity on the solutions to these equations. For comparative purposes, the equations were solved using δ_2 values of $\delta_2 \pm 0.005$, a reasonable error in the measured chemical shift of **2**-D_2. With $\delta_2 = 3.875$ (i.e., $\delta_1 - \delta_2 > \delta_0 - \delta_1$), the equations yielded the solution $\delta_b = 3.38$, $\delta_t = 4.205$, $K_1 = 0.375$, and $K_2 = 1.50$. Solving with $\delta_2 = 3.885$ (i.e., $\delta_1 - \delta_2 < \delta_0 - \delta_1$), the calculated values were $\delta_b = 4.38$, $\delta_t = 3.705$, $K_1 = 0.6875$, and $K_2 = 2.75$. The solutions are highly divergent. With $\delta_1 - \delta_2 > \delta_0 - \delta_1$, the chemical shift of the bridging BH appears upfield of the chemical shift of the terminal BH, but their positions are reversed for $\delta_1 - \delta_2 < \delta_0 - \delta_1$. The equilibrium constants favor H-bridging in the former, and D-bridging in the latter. Since one would expect chemical shifts of the terminal positions to be downfield of those corresponding to bridging positions and the K to favor μ-H over μ-D,[36] the first set of data are the better of the two guesses. However, the results appear unlikely for several reasons: (1) the two divergent solutions are within error of the shift measurement; (2) K_1 and K_2 represent large deviations from statistical values of 0.5 and 2.0, respectively (at 25 °C, $\Delta G°_1 - \Delta G°_{stat} = \Delta G°_2 - \Delta G°_{stat} = 189$ cal/mol; (3) the chemical shift differences between terminal and bridging sites are quite modest. While the $\Delta G°$ values appear small in magnitude, they are larger than bona fide cases of isotopic perturbation of chemical shift (e.g., $HOs_3(CO)_{10}(\mu_{1,2}$-H,C-$CH_3)$, $\Delta G° \approx$ 130 cal/mol;[33] $[Tp(PMe_3)Ir(H_2)H]BF_4$, $\Delta G° \approx 121$ cal/mol)[37] whose observed δ_n ($n = 0-2$ values were substantially greater than those for **2**-D_n and whose $\delta_1 - \delta_2 > \delta_0 - \delta_1$. The data, while inconclusive, support the unbridged, dative structure of **2**.

Discussion

General. The stability of **2** is remarkable in the context of the dehydrogenation of **5** and its lack of BH_3 transfer

(33) Shapley, J.; Calvert, R. B. *J. Am. Chem. Soc.* **1978**, *100*, 7726−7727.
(34) (a) Lambert, J. B.; Greifenstein, L. G. *J. Am. Chem. Soc.* **1974**, *96*, 5120−5124. (b) Luo, X. L.; Crabtree, R. H. *J. Am. Chem. Soc.* **1990**, *112*, 4813−4821.
(35) Carpenter, B. K. *Determination of Reaction Mechanisms*; Wiley-Interscience: New York, 1984.
(36) (a) Bigeleisen, J.; Mayer, M. G. *J. Chem. Phys.* **1947**, *15*, 261−267. (b) Melander, L.; Saunders, W. H. *Reaction Rates of Isotopic Molecules*; Wiley: New York, 1980.
(37) Heinekey, D. M.; Oldham, Jr., W. J. *J. Am. Chem. Soc.* **1994**, *116*, 3137−3138.

Table 1. Relative Conformational Energies (ΔE, kcal/mol) Pertaining to Calculational Models of $(RO)_3Ta(BH_3)$

OR	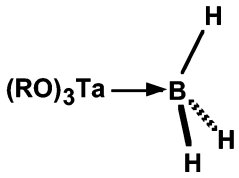	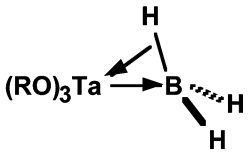	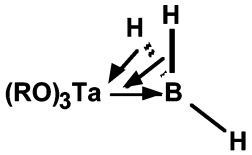
OH (**2'**)	[a]	[a]	0.0[b]
$OSiH_3$ ($\mathbf{2}^{SiH}$)	2.3	0.0	0.5
$OSiMe_3$ ($\mathbf{2}^{SiMe}$)	0.7	0.0	1.8
OSi^tBu_3 ($\mathbf{2}^{SiBu}$)	0.0	0.2	0.2[c]

[a] Rearranged to $(RO)_2Ta(\eta^3\text{-H,H,B-BH}_3)$ upon geometry optimization. [b] Only stable minimum obtained for **2′**. [c] Conformation converts upon geometry optimization to a transition state between dative, $(RO)_3Ta{\rightarrow}BH_3$ and $(RO)_2Ta(\eta^2\text{-H,B-BH}_3)$ structures.

capabilities. Unfortunately, the conformation of the BH_3 unit is still ambiguous, hence computational methods were employed in an effort to establish its ground state structure. As for the Cl_2BPh adduct, **3**, its η^2-B,Cl binding mode looks like an arrested oxidative addition of the B−Cl bond, hence calculations were utilized in examining some of the energetics surrounding this plausible event.

Computational Models of 2. 1. Ground State Structure. Density functional calculations (B3LYP/CEP_31G(d)) were conducted on $(RO)_3Ta(BH_3)$ with sequentially larger substituents (R = H, **2′**; SiH_3, $\mathbf{2}^{SiH}$ $SiMe_3$, $\mathbf{2}^{SiMe}$, and Si^tBu_3, $\mathbf{2}^{SiBu}$) in order to assess the relative importance of steric and electronic effects on structure and bonding. DFT geometry optimizations on the small models **2′** and $\mathbf{2}^{SiH}$ indicated a preference for structures with one and two η^2-B,H interactions, as Table 1 indicates. Since η^2-B,H conformers contain hydrogen atoms in close proximity to the metal and shorter calculated BH bonds than the inverse adduct, an increase in steric interactions should shift the energetic balance away from the η^2-B,H species and toward the purely dative geometry. This was corroborated by calculations that showed the single η^2-B,H (i.e., $(RO)_3Ta(\eta^2\text{-B,H-BH}_3)$) and dative (i.e., $(RO)_3Ta{\rightarrow}BH_3$) structures to be essentially degenerate when $\mathbf{2}^{SiMe}$ and $\mathbf{2}^{SiBu}$ were the models, and the "double η^2-B,H" structure, $(RO)_3Ta(\eta^3\text{-H,H,B-BH}_3)$) did not even constitute a minimum in $\mathbf{2}^{SiBu}$. Given the calculated energies, it can be reasonably assumed that the interconversion of η^2-B,H and inverse adduct structures is likely to have a very modest barrier, no matter which conformation represents the true ground state.

Optimized geometries of $(silox)_3Ta{\rightarrow}BH_3$ and $\mathbf{2}^{SiMe}$ are given in Figures 3 and 4, respectively, with the methyl groups removed for clarity. The *d*(TaB) in the "inverse adduct" is 2.22 Å compared to 2.18 Å for the η^2-B,H conformer. The B−H bond length of the η^2-B,H interaction is 1.27 Å, which is substantially longer than the terminal BH bond distances of 1.21−1.23 Å. Aside from the asymmetry of the η^2-B,H conformation, the core geometries appear similar.

2. Electronic Structure of $\mathbf{2}^{SiBu}$. Figure 5 illustrates the d-orbital splitting diagrams of $(silox)_3Ta{\rightarrow}BH_3$ and $\mathbf{2}^{SiBu}$ and their respective TaB bonding orbitals. It is clear from either depiction that **2** can be considered a d^0 species, since the

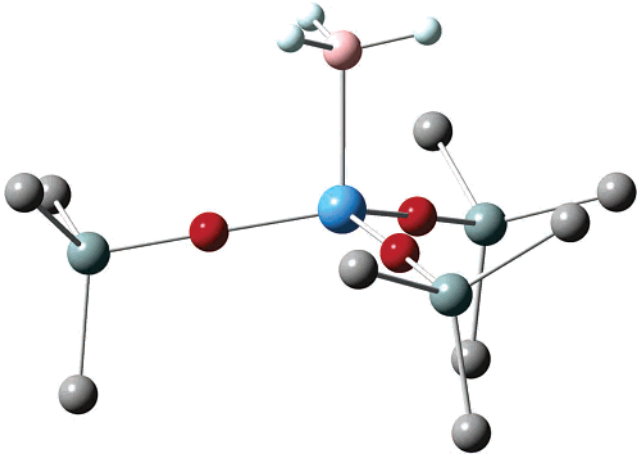

Figure 3. DFT-optimized geometry of "inverse adduct" conformer of $(silox)_3Ta{\rightarrow}BH_3$ ($\mathbf{2}^{SiBu}$); methyl groups have been omitted for clarity. Interatomic distances (Å) and angles (deg): TaB = 2.22; BH = 1.23; Ta···H = 2.78−2.80; O−Si = 1.71; Ta−O = 1.89; Ta−O−Si = 179; TaBH = 104−105; O−Ta−B = 100 −101; O−Ta−O = 117.

TaB bonding orbitals are very low in energy and their corresponding σ^* orbitals are in the energy realm of the remaining d orbitals. For the "inverse-adduct" model, the TaB σ^b orbital is at −5.5 eV, well below the TaO π^* orbitals at −1.0 eV (d_{xz}, d_{yz}) and the TaO σ^* orbitals at 0.2 eV ($d_{x^2-y^2}$, d_{xy}) and 0.3 eV ("d_{z^2}", i.e., TaB σ^*). To further probe the nature of the TaB bond in $(silox)_3Ta{\rightarrow}BH_3$, a natural bond orbital (NBO) analysis was conducted on the more computationally tractable $\mathbf{2}^{SiMe}$. It indicates a covalent TaB bond that is 55% Ta and 45% B (primarily 2p) in character, with the tantalum contribution split 50:50 between 6s and $5d_{z^2}$.

The orbitals pertaining to the model $\mathbf{2}^{SiBu}$ are quite similar but with greater delocalization, as expected. The lowest orbital at −5.4 eV manifests the TaB bonding, and the next two are TaO π^* orbitals at −1.0 and −0.8 eV (d_{xz}, d_{yz}). One of the TaO σ^* orbitals ($d_{x^2-y^2}$) now possesses additional TaBH σ^* character and is raised to 0.5 eV relative to its partner d_{xy} at 0.1 eV. An orbital that appears to be mostly TaB antibonding in character resembling d_{z^2} is found at 0.3 eV.

3. Vibrational Structure. In an effort to discern the η^2-B,H ground state from the "inverse adduct" conformer pertaining to **2**, IR spectra were first calculated on $\mathbf{2}^{SiMe}$. The

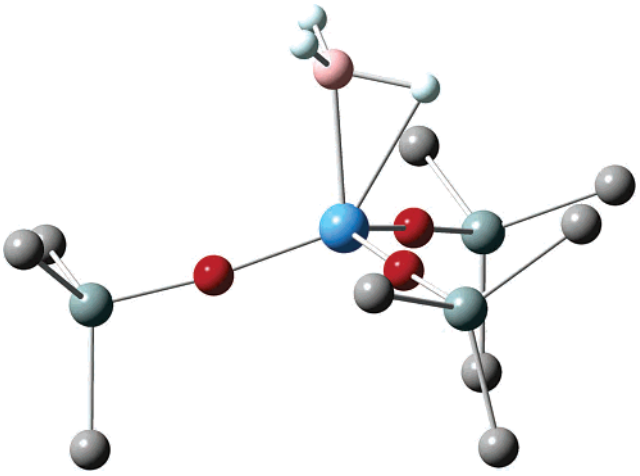

Figure 4. DFT-optimized geometry of the η^2-B,H conformer of (silox)$_3$-Ta(η^2-H,B-BH$_3$) (**2**^{SiBu}); methyl groups have been omitted for clarity. Interatomic distances (Å) and angles (deg): TaB = 2.18; BH$_t$ = 1.21; BH$_b$ = 1.27; Ta···H$_t$ = 2.91 and 2.93; TaH$_b$ = 2.22; O−Si = 1.70−1.71; Ta−O = 1.88−1.90; Ta−O−Si = 174−176; TaBH$_t$ = 116 and 117; TaBH$_b$ = 75; O−Ta−B = 100−106; O−Ta−O = 112−122.

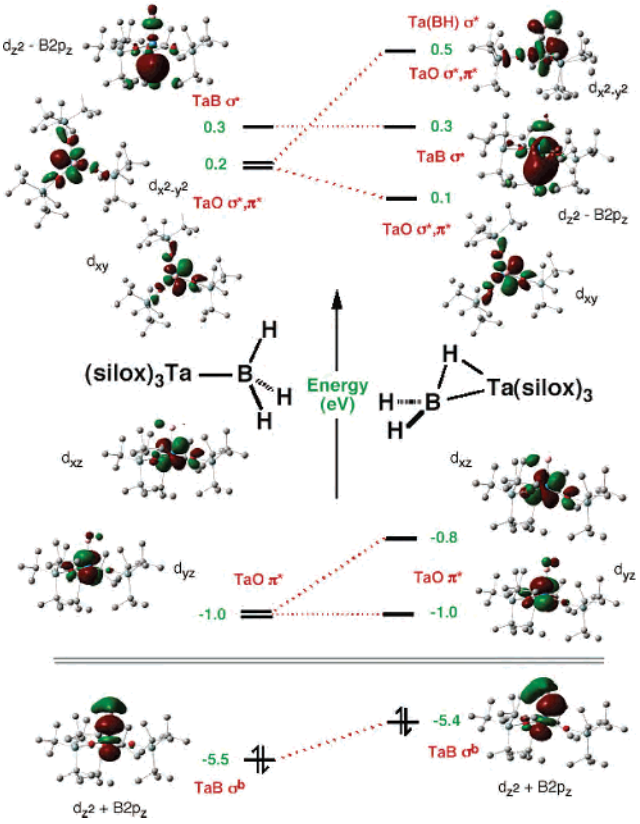

Figure 5. d-Orbital splitting diagrams plus the TaB bonding orbital for calculational models (silox)$_3$Ta−BH$_3$ and (silox)$_3$Ta(η^2-H,B-BH$_3$) (**2**^{SiBu}); some hydrogens have been omitted.

main group adduct, Me$_3$N→BH$_3$, was chosen to calibrate computational vs experimental vibrational data because the true structures of plausible transition metal candidates were unknown.[2−5] Carpenter and Ault[38] reported B−H stretching frequencies of 2367 (ν_a, ^{11}B) and 2270 cm^{-1} (ν_s, ^{11}B) for Me$_3$NBH$_3$ in an argon matrix, while gas-phase geometry optimization and energy Hessian calculations for the same at the B3LYP/CEP_31G(d) level of theory yielded values of 2466 (ν_a) and 2408 cm^{-1} (ν_s) for ^{11}B−H stretches, implicating scaling factors of 0.96 (ν_a(^{11}BH)) and 0.94 (ν_s(^{11}BH)) to compensate for anharmonic effects, the incomplete basis set, etc.[39] For the purely dative conformer of **2**^{SiBu}, the calculated stretching frequencies are 2454 cm^{-1} (actually 2451 and 2457 cm^{-1} due to deviation from strict C_{3v} symmetry in the computation) for ν_a(^{11}BH) and 2392 cm^{-1} for ν_s(^{11}BH), with a 4:1 intensity ratio; the scaled bands are at 2355 and 2248 cm^{-1}. The η^2-B,H conformer has 2558 (ν_a(^{11}BH)) and 2496 cm^{-1} (ν_s(^{11}BH)) absorptions in a 2:1 ratio that scale to 2456 and 2346 cm^{-1}. The latter more closely agrees with the 2445 and 2395 cm^{-1} absorptions present in a nujol mull of **2**.[40] The calculated η^2-B,H structure of **2**^{SiBu} also possesses a stretch for the bridging Ta···HB at 2139 cm^{-1}, which should have an intensity in between the terminal bands and would scale to roughly 2150−2010 cm^{-1}, provided the previous scale factors were applicable. In reinvestigating the experimental IR spectrum of **2**, an asymmetric absorption at ∼2030 cm^{-1} can be seen, although it is very broad, spanning a 2250−1950 cm^{-1} range. The presence of this broad absorption and the nearly matching frequencies of **2**^{SiBu} and the experimental spectrum of **2** suggest that the η^2-B,H conformer is the ground state structure.

With the vibrational structure of **2**^{SiBu} in hand, the energy difference between (silox)$_3$Ta(η^2-B,H-BH$_2$D) and (silox)$_3$-Ta(η^2-B,D-BH$_2$D) (**2**^{SiBu}-D) could be calculated by simple placement of deuterium in the model. At 296 K, the η^2-B,H, D-terminal structure was calculated to be more favorable than the η^2-B,D, H-terminal isotopomer by −78 cal/mol. This modest value is consistent with the inability of the isotopic perturbation of chemical shift experiment to discern the η^2-B,H structure, assuming the chemical shifts of η^2-B,H and terminal positions are not hugely different.

4. BH$_3$ Binding Energies. The binding energy of BH$_3$ to (RO)$_3$Ta was calculated for R = SiH$_3$ (**2**^{SiH}) and SiMe$_3$ (**2**^{SiMe}). For both models the binding energy is exothermic by ≥35 kcal/mol to either the η^2-B,H or purely dative structures. Given the similarity in binding energies for the two models, calculations employing the post-Hartree−Fock coupled clusters methodology (i.e., CCSD(T)/CEP-31G(d)//B3LYP/CEP-31G(d)) were conducted on the smaller of the two (**2**^{SiH}) to assess the binding energy at this more extensive electron correlation level. These calculations afforded comparable binding energies (∼ −35 to −37 kcal/mol depending on borane conformation) and are fully consistent with the stability accorded **2**.

Both η^2-B,H and "inverse adduct" structures confer substantial stability to a dative interaction that can be construed as having considerable covalent character (i.e., Ta$^+$−BH$_3^-$). It is tempting to assign a Ta(V) oxidation state

(38) Carpenter, J. D.; Ault, B. S. *J. Phys. Chem.* **1991**, *95*, 3507−3511.

(39) Several, groups, most notably that of Pulay, have discussed the appropriateness of having different scale factors for different vibrational modes. See: Rauhut, G.; Pulay, P. *J. Phys. Chem.* **1995**, *99*, 3093−3100.

(40) Using a single, averaged scaling factor of 0.95 does not change these conclusions and actually makes the predicted IR bands for the η^2-B,H conformer much closer to the observed.

Table 2. Comparison of Experimental and Calculational Metric Parameters Pertaining to (silox)$_3$Ta(η^2-B,Cl-BCl$_2$Ph) (**3** and **3**^{SiBu})[a]

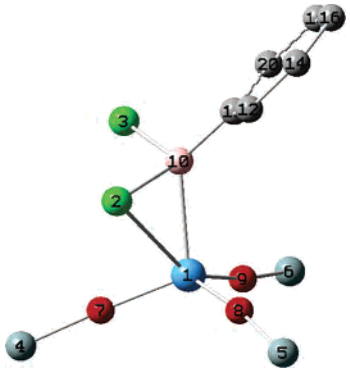

bonds	(Å, calcd)	(Å, exptl)	angles	(deg, calcd)	(deg, exptl)
Ta(1)−O(7)	1.907	1.885(4)	Ta(1)−O(7)−Si(4)	172.7	173.6(3)
Ta(1)−O(8)	1.898	1.890(4)	Ta(1)−O(8)−Si(5)	172.6	168.6(3)
Ta(1)−O(9)	1.890	1.875(5)	Ta(1)−O(9)−Si(6)	172.4	168.6(3)
O(7)−Si(4)	1.725	1.693(5)	O(7)−Ta(1)−B(10)	109.6	108.4(2)
O(8)−Si(5)	1.732	1.699(4)	O(8)−Ta(1)−B(10)	107.0	109.4(2)
O(9)−Si(6)	1.739	1.702(5)	O(9)−Ta(1)−B(10)	102.0	101.2(2)
Ta(1)−B(10)	2.324	2.308(8)	O(7)−Ta(1)−O(8)	121.2	123.5(2)
B(10)−Cl(2)	2.029	1.999(8)	O(7)−Ta(1)−O(9)	106.3	105.4(2)
B(10)−Cl(3)	1.875	1.828(8)	O(8)−Ta(1)−O(9)	109.0	106.6(2)
B(10)−C(11)	1.596	1.582(11)	Ta(1)−B(10)−Cl(2)	76.1	72.6(3)
			Ta(1)−B(10)−Cl(3)	111.1	114.7(4)
			Ta(1)−B(10)−C(11)	129.0	126.4(5)
			Cl(2)−B(10)−Cl(3)	108.1	107.5(4)
			Cl(2)−B(10)−C(11)	111.7	110.9(5)
			Cl(3)−B(10)−C(11)	113.2	114.4(5)

[a] ^{t}Bu groups have been removed from the silox ligand for clarity.

to **2** on the basis of its stability, but there is little calculational support for a formal Ta^{2+}←BH_3^{2-} distribution of charge. The tantalum is not considered formally oxidized to Ta(V), but its *valence*—the number of tantalum electrons utilized in bonding—is five. As Parkin has argued,[20,23] despite a formal oxidation state of (III) for the tantalum, it is a d^0 center on the basis of valence, the same as it is in the formally Ta(V) hydride-borohydride, **5**. The molecular orbital diagrams support this depiction, since $5e^-$ from tantalum are utilized in bonding orbitals that lie well below the d-block in energy.

5. Calculated NMR Parameters. ^{1}H NMR chemical shifts were calculated for the η^2-B,H and dative conformers of **2**^{SiMe} using the gauge-independent atomic orbital (GIAO)[41] method and the B3LYP functional. For the main group elements, the extended Pople basis set 6-311+G(2d,p) was used, while the triple-ζ CEP-31G valence basic set/effective core potential was maintained for tantalum. In the "inverse adduct" conformer, a chemical shift of δ 2.7 was calculated for the three equivalent hydrogens. The η^2-B,H conformer of **2**^{SiMe} is calculated to have a shift of δ 2.1 for the bridging proton and δ 4.2 for the terminal protons, yielding a weighted average of δ 3.5, which is marginally closer to the experimental shift of δ 3.9. Calculations of J_{BH} proved to be equally insufficient at differentiating dative (J_{BH} = 101 Hz) and η^2-B,H ($J_{BH}(BH_b)$ = 59 Hz, $J_{BH}(BH_t)$ = 118 Hz; J_{BH}(ave) = {59 + 2(118)}/3 = 98 Hz) structures, although both were quite close to the experimental value of 98 Hz. Despite a reasonable calibration with known compounds (e.g., BH_4^-, BCl_3, B_2H_6, BF_3•OEt_2), the ^{11}B NMR shifts calculated for the η^2-B,H (δ 8) and dative (δ −3) structures are not close to the observed value of δ 28, which is midrange between related BX_3 (sp^2, δ 60−80) and BX_4^- (sp^3, δ −20) species.[42]

Computational Model of 3. Table 2 lists the experimental core distances and angles referenced to those calculated for the model (silox)$_3$Ta(η^2-B,Cl-BCl$_2$Ph) (**3**^{SiBu}), and there is excellent agreement between them. The worst distance comparison is for the terminal B−Cl bond, where the calculated bond length is ∼0.05 Å greater than the 1.83 Å observed, and most are within 0.03 Å. The same is true for the bond angles, where the worst cases are still within ∼4° of the experimental values.

Initial B3LYP/CEP-31G(d) optimization of (RO)$_3$Ta(BCl$_2$-Ph) using R = H (**3′**), SiH_3 (**3**^{SiH}), and $SiMe_3$ (**3**^{SiMe}) yielded a trigonal bipyramidal boryl complex, d^0 (RO)$_3$ClTaBClPh. In following the course of geometry optimizations, a shallow minimum was observed in the vicinity of a (RO)$_3$Ta(η^2-B,Cl-BCl$_2$Ph) structure, which eventually stabilized through B−Cl bond lengthening to afford the oxidative addition product, the boryl-chloride. It was only until the full silox model (R = Si^{t}Bu, **3**^{SiBu}) was employed that the η^2-B,Cl adduct became stable. The results imply that the unusual geometry of **3** is a consequence of the severe steric interactions of the silox groups, which effectively arrest the B−Cl oxidative addition.

(41) Gauss, J.; Stanton, J. F. *Adv. Chem. Phys.* **2002**, *123*, 355−422.

(42) Hermánek, S. *Chem. Rev.* **1992**, *92*, 325−362.

Conclusions

The treatment of **1** with BH_3 and BCl_2Ph afforded two adducts in which the principal interaction is a donation from the filled d_{z^2} orbital of the d^2 tantalum center to the empty $2p_z$ orbital of boron that is covalent in nature. The conformation of **2** could not be confirmed despite exhaustive spectroscopic studies and the isotopic perturbation of chemical shift investigation, but calculations on (silox)$_3$Ta(η^2-B,H-BH_3) and (silox)$_3$Ta→BH_3 (**2**^{SiBu}) provided vibrational frequencies that more closely match that of the former η^2-B,H structure. The η^2-B,H structure is favored as the GS geometry in models containing small RO (R = H, SiH_3, $SiMe_3$) but the "inverse-adduct" conformer becomes energetically competitive as the steric parameters are increased to R = ^{t}Bu$_3$Si because its Ta−B bond is longer than in the η^2-B,H species. The similar energies accorded the two conformations suggest that their dynamic interconversion is quite likely. The stabilization of the pair of electrons in the Ta→B bond renders the tantalum effectively d^0 and energetically competitive with any BH oxidative addition product.

Steric influences dramatically affect the binding of Cl_2-BPh as well. According to the calculations, a trigonal bipyramidal oxidative addition product, (RO)$_3$ClTaBClPh, becomes less favored with respect to the (RO)$_3$Ta(η^2-B,Cl-BCl_2Ph) adduct as the size of RO (R = H, **3′**; SiH_3, **3**^{SiH}; $SiMe_3$, **3**^{SiMe}; Si^{t}Bu$_3$, **3**^{SiBu}) is increased. It is somewhat surprising that the steric features of silox push the equilibrium away from a formal Ta(V) oxidative addition product to the μ-Cl adduct, **3**. In this structure, the tantalum can be considered d^0 as it contributes $2e^-$ to the Ta→B dative bond, and a strong B−Cl bond is retained. These factors and the steric influence of silox help counteract the tendency toward oxidative addition of the BCl bond. This is the first time calculations have indicated that steric features of silox changed the reactivity at the metal center aside from preventing dimerization.

Experimental Section

General Considerations. All manipulations were performed using either glovebox or high vacuum line techniques. All glassware was oven-dried. THF and ether were distilled under nitrogen from purple sodium benzophenone ketyl and vacuum-transferred from the same prior to use. Hydrocarbon solvents were treated in the same manner with the addition of 1−2 mL/L tetraglyme. Benzene-d_6 was dried over sodium, activated 4 Å molecular sieves, vacuum-transferred, and stored under nitrogen. THF-d_8 was dried over sodium and vacuum-transferred from sodium benzophenone ketyl prior to use. H_2 and D_2 were passed over a column containing activated 4 Å sieves and copper oxide. BH_3·THF, $PhBCl_2$, and $LiBD_4$ were purchased from Aldrich and used without further purification. B_2D_6 was prepared by adding I_2/tetraglyme solution to $NaBD_4$ in tetraglyme. D_2 was separated by freeze(77K)/pump/thaw degassing. Pure B_2D_6 was then transferred to a separate bomb and stored at 77 K. **1**[24] and **4**[30] were prepared following published procedures.

^{1}H, ^{13}C{^{1}H}, and ^{11}B NMR spectra were obtained on Varian XL-200 and XL-400 spectrometers. Chemical shifts are reported relative to benzene-d_6 (^{1}H, δ 7.15; ^{13}C{^{1}H}, δ 128.00) and BF_3·OEt_2 (^{11}B, δ 0.00). IR spectra were recorded on a Mattson FT-IR, Perkin-Elmer 299B grating IR, or PE 377 grating IR. Cryoscopic molecular weight determination in benzene was performed with a homemade device. Combustion analyses were performed by Oneida Research Services (Whitesboro, NY), Robertson Microlit Laboratories (Madison, NJ), or Texas Analytical (Houston, TX).

Syntheses. 1a. (silox)$_3$Ta(BH$_3$) (2). A 25 mL two-neck flask was charged with 0.251 g of **1** (0.303 mmol), fitted with a septum, and attached to a frit assembly. The apparatus was evacuated, and Et_2O (10 mL) was added via vacuum-transfer at −78 °C. The frit assembly was filled with Ar, and 0.31 mL of 1.0 M (in THF, 0.31 mmol) BH_3·THF was syringed into the cold solution. The blue color was discharged immediately, and the resulting orange solution was allowed to warm to 23 °C and was stirred for 30 min. After the septum was replaced with a glass stopper, the volatiles were removed in vacuo and the solid residue was dissolved in hexane. Filtration, concentration to 3 mL, and cooling to −78 °C generated pale orange crystals which were collected by filtration (0.141 g). A second crop yielded 0.031 g (67% total). ^{1}H NMR (C_6D_6) δ 1.28 (s, ^{t}Bu, 81H), 3.93 (br quar, BH_3, $^1J_{BH}$ = 98 Hz, 3H); (THF-d_8) δ 1.25, 3.30. ^{13}C{^{1}H} NMR (C_6D_6) δ 23.78 (Si*C*), 30.48 (C(*C*H$_3$)$_3$); (THF-d_8) δ 24.36, 30.88. ^{11}B NMR (C_6D_6) δ 27.89 (quar, $^1J_{BH}$ = 98 Hz); (THF-d_8) δ 32.52. IR (nujol, cm^{-1}) 2445 (br m), 2395 (br m), 2030 (v br), 1475 (s), 1375 (s), 1290 (w), 1010 (m), 930 (s), 860 (br, s), 810 (s), 665 (w), 620 (s), 585 (m). M_r found: 833(25); calcd: 841. Anal. Calcd for $C_{36}H_{84}BO_3Si_3Ta$: C, 51.41; H, 10.07. Found: C, 51.21; H, 10.23.

b. (silox)$_3$TaBD$_3$ (2-D$_3$). A sample of **1** (0.101 g, 0.122 mmol) was placed in a 10 mL flask, which was then attached to a gas bulb. THF (5 mL) was added at −78 °C, and the flask was cooled to 77 K. B_2D_6 (12.3 Torr in 91 mL, 0.061 mmol, 0.5 equiv) was condensed into the flask. Upon warming to −78 °C, the stirred solution quickly turned from blue to orange. Stirring was maintained for 1 h at −78 °C and for an additional 30 min at 23 °C. The THF was removed in vacuo, and hexane (2 × 5 mL) was placed on the orange solid and removed. The resulting material was judged >95% pure and >98% deuterated by a ^{1}H NMR assay and was used for IR studies without purification. IR (nujol, cm^{-1}, BD vibrations) 1845 (s), 1770 (s), 980 (s).

2. (silox)$_3$Ta(η^2-B,Cl-BCl$_2$Ph) (3). Into a two-neck flask was placed 0.499 g of **1** (0.603 mmol). A sidearm addition tube was charged with $PhBCl_2$ (78.3 μL, 0.603 mmol). The flask was cooled and evacuated, and 15 mL of toluene was added at −78 °C. The solution was warmed to 23 °C, and the $PhBCl_2$ was washed into the flask by condensing toluene into the sidearm. After 1 h the solution was filtered, and the volume of the filtrate reduced to 5 mL. After cooling to −78 °C, small portions of hexane (~1 mL total) were added until copious solid was observed. Orange crystals were collected by filtration and washed with cold hexane (0.409 g, 69%). ^{1}H NMR (C_6D_6) δ 1.26 (s, ^{t}Bu, 81H), 7.02 (t, *p*-H, 1H), 7.33 (t, *m*-H, 2H), 7.95 (d, *o*-H, 2H). ^{13}C{^{1}H} NMR (THF-d_8) δ 24.42 (Si*C*), 31.33 (C(*C*H$_3$)$_3$), 126.59, 128.22, 134.99 (Ph), B*C*(ipso) not observed. ^{11}B NMR (C_6D_6) δ 61.79 (br s). IR (nujol, cm^{-1}) 1475 (s), 1375 (m), 1190 (m), 1175 (m), 1150 (w), 1035 (w), 1015 (m), 935 (br, s), 870−750 (br, s), 725 (s), 700 (m), 625 (s). Anal. Calcd for $C_{42}H_{86}BCl_2O_3Si_3Ta$: C, 51.16; H, 8.79. Found: C, 51.29; H, 9.03.

3a. (silox)$_3$HTa(η^3-BH$_4$) (5). A 0.236 g sample of **1** (0.285 mmol) was placed in a 25 mL two-neck flask. The flask was fitted with a stopper, attached to a frit, and cooled to −78 °C. Diethyl ether (15 mL) was added by vacuum transfer, and the frit was filled with dry H_2 (~600 Torr). The solution was stirred for 11 h at 23 °C until all vestiges of blue color disappeared. The excess H_2 was removed, and a septum was attached to the flask under Ar

counterflow. BH_3·THF (0.28 mL, 1 M in THF, 0.28 mmol) was added via syringe to the ether solution at −78 °C. The flask was allowed to warm to 23 °C, and stirring was maintained for 1.5 h. The volatiles were removed, and the volume of the solution was reduced to 10 mL. Filtration was followed by further concentration to 3 mL, and cooling to −78 °C generated a white crystalline solid that was isolated by filtration (0.186 g, 77%). ^{1}H NMR (C_6D_6) δ 1.29 (s, ^{t}Bu, 81H), 3.48 (br quar, BH_4,$^1J_{BH}$ = 88 Hz, 4H), 22.47 (br quin, TaH,$^2J_{HH}$ = 12 Hz, 1H). ^{13}C{^{1}H} NMR (C_6D_6) δ 24.25 (Si*C*), 30.47 (C(*C*H$_3$)$_3$). ^{11}B NMR (C_6D_6) δ −16.72 (quin,$^1J_{BH}$ = 88 Hz). IR (nujol, cm^{-1}) 2495 (m), 2200 (br, m), 2150 (br, m), 1765 (br, s), 1470 (s), 1375 (m), 1160 (br, w), 1010 (w), 960 (w), 925 (w), 870 (br, s), 810 (s), 620 (s). Anal. Calcd for $C_{36}H_{86}BO_3Si_3Ta$: C, 51.29; H, 10.28. Found: C, 51.57; H, 10.50.

b. (silox)$_3$DTa(η^3-BD$_4$) (5-D$_5$). Into a 10 mL flask was placed **1** (0.102 g, 0.123 mmol). The flask was attached to a gas bulb, evacuated, and cooled to −78 °C. THF (5 mL) was added followed by 600 Torr of D_2. The solution was stirred for 1 h at 23 °C and freeze/pump/thaw degassed. The reaction was recharged with D_2 and stirred for another 1.5 h. After the solution was degassed, B_2D_6 (13.5 Torr in 91 mL, 0.067 mmol, 0.54 equiv) was condensed into the flask. The solution was stirred for 3 h, and the volatiles were removed. The white solid obtained after addition and removal of 2 × 5 mL hexane was found to be >95% pure and ∼60% deuterated (Ta−H and BH_4 sites), which was sufficient for the IR study. IR (nujol, cm^{-1}, B−D and Ta−D vibrations) 1870, 1630, 1580, 1270 (TaD).

NMR Tube Reactions. 4. 2 + C_2H_4. An NMR tube attached to a ground glass joint was charged with **2** (0.018 g, 0.021 mmol) and attached to a gas bulb. C_6D_6 (0.6 mL) was added at 77 K followed by C_2H_4 (57.4 Torr in 20.5 mL, 0.064 mmol, 3 equiv). The tube was sealed with a torch under dynamic vacuum. No change was noted in the ^{1}H NMR spectrum of the sample after weeks at room temperature and 20 h at 90 °C.

5. 2 + Me_3N. An NMR tube on a 14/20 joint was charged with a sample of **2** (0.010 g, 0.012 mmol). The tube was attached to a gas bulb and evacuated. Benzene-d_6 (0.6 mL) and Me_3N (188 Torr in 12.3 mL, 0.126 mmol, 10.5 equiv) were added at 77 K. The tube was flame-sealed under dynamic vacuum. After a week at room temperature, the NMR spectrum showed only **2** and Me_3N.

6. 5 + Me_3N. A 25 mL flask containing an ether solution of **4** (0.052 g, 0.063 mmol) was treated with BH_3·THF (0.063 mL, 1 M in THF, 0.063 mmol) and stirred for 18 h. The volatiles were removed, and the NMR spectrum of the resulting solid showed only **5**. The solid was transferred into an NMR tube on a ground glass joint with 0.7 mL of C_6D_6. The tube was attached to a gas bulb and freeze/pump/thaw degassed three times. Me_3N (55.2 Torr in 20.5 mL, 0.062 mmol) was condensed into the tube, which was sealed with a torch. The ^{1}H NMR spectrum taken immediately upon warming showed a 1:1 mixture of **4** and **5**. Within 3 h, the NMR showed no **5** and complete formation of the products, **4** and Me_3N·BH_3.

7. 2 + BH_3·THF. To an NMR tube attached to a ground glass joint was added a sample of **2** (0.012 g, 0.014 mmol). The tube was attached to a 180° needle valve and freeze/pump/thaw degassed. THF-d_8 (0.6 mL) was added via vacuum-transfer. Against a counterflow of N_2, BH_3·THF (14 μL, 1 M in THF, 0.014 mmol) was added to the tube. After degassing, the tube was frozen at 77 K and flame-sealed under dynamic vacuum. The room-temperature ^{11}B NMR spectrum of this sample showed a sharp quartet at δ 30.5 for **2** and a broad signal at δ −0.1 corresponding to BH_3·THF, neither of which showed any sign of coalescing or broadening up to 80 °C.

8. 5 + D_2. A sample of **5** was placed into an NMR tube attached to a 14/20 joint. The tube was fixed to a 180° needle valve and evacuated. C_6D_6 (0.6 mL) was added via vacuum-transfer. The tube was filled with ∼600 Torr of D_2 and sealed with a torch. After thermolysis at 90 °C for 18 h, the ^{1}H{^{11}B} NMR spectrum showed the presence of **2**, **2**-D, and **2**-D_2.

Single-Crystal X-ray Structure Determination. 9. 3. An orange crystal approximately 0.4 × 0.5 × 0.4 mm^3 obtained from a toluene/hexane solution was mounted in a capillary and placed in the goniometer of a Siemens *P*4 diffractometer equipped with a fine-focus molybdenum X-ray tube and graphite monochromator at 293-(2) K. Preliminary diffraction data revealed a triclinic cell, a hemisphere routine was used to collect the data, and precise lattice constants (a = 13.1510(1) Å, b = 13.1990(10) Å, and c = 17.441-(2) Å; a = 102.020(10)°, b = 96.160(10)°, g = 119.120(10)°; V = 2508.5(4) Å^3) were determined from a least-squares fit of 15 measured 2θ values. The space group ($P\bar{1}$) was determined, and after correction for Lorentz, polarization, and background effects, unique data were judged observed according to $|F_o| > 2\sigma|F_o|$ (6444 out of 7476; 464 parameters). All heavy atoms were located using direct methods, and all non-hydrogen atoms were revealed by successive Fourier syntheses. Full matrix, least-squares refinements (minimization of $\sum w(F_o - F_c)^2$ where w is based on counting statistics modified by an ignorance factor, w^{-1}) with anisotropic heavy atoms and all hydrogens included at calculated positions led to the final model. Refinement utilized SHELXL and $w^{-1} = \sigma^2(F_o^2) + (0.0595p)^2 + 7.1714p$, where $p = (F_o^2 + 2F_c^2)/3$). R1 [$I > 2\sigma(I)$] = $\sum||F_o| - |F_c||/\sum|F_o|$ = 0.0433, R1 (all data) = 0.0560; wR2 [$I > 2\sigma(I)$] = $[\sum w(|F_o| - |F_c|)^2/\sum wF_o^2]^{1/2}$ = 0.1047, wR2 (all data) = 0.1174; GOF (all data, n = number of independent reflections, p = number of parameters) = $[\sum w(|F_o| - |F_c|)^2/(n - p)]^{1/2}$ = 1.040.

Computational Methods. All calculations were carried out using the Gaussian03[43] suite of programs. The B3LYP functional (Becke's three-parameter hybrid functional[44] using the LYP correlation functional containing both local and nonlocal terms of Lee, Yang, and Parr)[45] and VWN (Slater local exchange functional[43] plus the local correlation functional of Vosko, Wilk, and Nusair)[46] was employed in conjunction with the CEP-31G(d) valence basis sets and effective core potentials of Stevens et al.[47] Closed-shell (diamagnetic) and open-shell (paramagnetic) species were modeled within the restricted and unrestricted Kohn−Sham formalisms,[48] respectively. All systems were fully optimized without symmetry constraint.

(43) Frisch, M. J.; Trucks, G. W.; Schlegel, H. B.; Scuseria, G. E.; Robb, M. A.; Cheeseman, J. R.; Montgomery, J. A., Jr.; Vreven, T.; Kudin, K. N.; Burant, J. C.; Millam, J. M.; Iyengar, S. S.; Tomasi, J.; Barone, V.; Mennucci, B.; Cossi, M.; Scalmani, G.; Rega, N.; Petersson, G. A.; Nakatsuji, H.; Hada, M.; Ehara, M.; Toyota, K.; Fukuda, R.; Hasegawa, J.; Ishida, M.; Nakajima, T.; Honda, Y.; Kitao, O.; Nakai, H.; Klene, M.; Li, X.; Knox, J. E.; Hratchian, H. P.; Cross, J. B.; Bakken, V.; Adamo, C.; Jaramillo, J.; Gomperts, R.; Stratmann, R. E.; Yazyev, O.; Austin, A. J.; Cammi, R.; Pomelli, C.; Ochterski, J. W.; Ayala, P. Y.; Morokuma, K.; Voth, G. A.; Salvador, P.; Dannenberg, J. J.; Zakrzewski, V. G.; Dapprich, S.; Daniels, A. D.; Strain, M. C.; Farkas, O.; Malick, D. K.; Rabuck, A. D.; Raghavachari, K.; Foresman, J. B.; Ortiz, J. V.; Cui, Q.; Baboul, A. G.; Clifford, S.; Cioslowski, J.; Stefanov, B. B.; Liu, G.; Liashenko, A.; Piskorz, P.; Komaromi, I.; Martin, R. L.; Fox, D. J.; Keith, T.; Al-Laham, M. A.; Peng, C. Y.; Nanayakkara, A.; Challacombe, M.; Gill, P. M. W.; Johnson, B.; Chen, W.; Wong, M. W.; Gonzalez, C.; Pople, J. A. *Gaussian 03*, revision C.02; Gaussian, Inc.: Wallingford, CT, 2004.
(44) Becke, A. D. *J. Chem. Phys.* **1993**, *98*, 1372−1377.
(45) Lee, C.; Yang, W.; Parr, R. G. *Phys. Rev.* **1998**, *B37*, 785.
(46) Vosko, S. H. W., L.; Nusair, M. *Can. J. Chem.* **1980**, *58*, 1200.
(47) (a) Stevens, W. J.; Basch, H.; Krauss, M. *J. Chem. Phys.* **1984**, *81*, 6026−6033. (b) Stevens, W. J.; Basch, H.; Krauss, M.; Jasien, P. G. *Can. J. Chem.* **1992**, *70*, 612−630.

Acknowledgment. P.T.W. thanks the NSF (CHE-0415506) and Cornell University, and T.R.C. thanks the DOE (No. DEFG02-03ER15387) for research support. The U.S. Department of Education is acknowledged for support of the CASCaM facility, and the NSF (CHE-0342824) for support of the UNT computational chemistry resource. A.W.P. acknowledges the UNT Toulouse School of Graduate Studies for a fellowship. We thank Elliott B. Hulley for experimental assistance.

Supporting Information Available: Crystallographic data in cif format. This material is available free of charge via the Internet at http://pubs.acs.org.

IC0616885

(48) Kohn, W.; Sham, L. *Phys. Rev.* **1980**, *A140*, 1133−1138.